ACCELERATING TURBULENT PIPE FLOW: ROLE OF THE LARGE- AND SMALL-SCALES OF MOTION

Byron Guerrero
School of Mechanical Engineering
University of Adelaide
Adelaide SA 5000, Australia
byron.guerrerohinojosa@adelaide.edu.au

Martin F. Lambert
School of Civil and Environmental Engineering
University of Adelaide
Adelaide SA 5000, Australia
martin.lambert@adelaide.edu.au

Rey C. Chin
School of Mechanical Engineering
University of Adelaide
Adelaide SA 5000, Australia
rey.chin@adelaide.edu.au

ABSTRACT

This paper examines the time response of the transient turbulent dynamics of an accelerating turbulent pipe flow using direct numerical simulation (DNS) data sets. A low/high-pass Fourier filter is used to investigate the contribution and time dependence of the large- (LSM) and the small-scale motions (SSM) into the Reynolds shear stress. Additionally, it is analysed how the LSM and SSM influence the mean wall shear stress through the so-called FIK identity (Fukagata *et al.*, 2002). The results reveal that turbulence is largely frozen during the early flow excursion. During the pre-transitional stage, an energy growth of the LSM and a subtle decay in the SSM is observed, suggesting a laminarescent trend of small-scale turbulence during this period. The transitional stage exhibits a rapid energy growth in the SSM spectrum at the near-wall region, which is the dominant contribution to the frictional drag. Finally, the core-relaxation stage shows a quasi-steady behaviour in large-and small-scale turbulence at the near-wall region and progressive growth of small- and large-scale turbulence within the wake region.

INTRODUCTION

Turbulent pipe flows have been studied for about 140 years, starting from the seminal investigation conducted by Reynolds (1883). Most of the existing studies concerning turbulent pipe flow in smooth and rough walls have been performed assuming steady turbulence conditions (i.e. constant flow rate). These studies have provided an essential understanding for estimating essential flow quantities, such as the mean skin friction coefficient. A suitable prediction of the steady-state skin fric-

tion coefficient allows quantifying the energy dissipation in a fluid transportation system at a constant flow rate. Nonetheless, fluid transportation through pipes is seldom steady. Indeed, the flow rate within a pipe is constantly modulated by control valves or pumping systems to fulfil the system's demands. As a result, industrial pipe flows are constantly experiencing accelerations and decelerations. However, transient turbulent pipe flows have received little attention in comparison. Hence a more profound understanding of the flow physics in unsteady (i.e. accelerating and decelerating) turbulent pipes becomes necessary to quantify and predict the transient energy dissipation.

In this paper we will focus on accelerating turbulent pipe flows. One of the interesting characteristics of accelerating turbulent pipe flows is that turbulence generation and propagation experiences a delay concerning the increase in the flow rate (Maruyama *et al.*, 1976). In fact, during the early flow excursion, turbulence exhibits a 'frozen' behaviour. Later, there exists a second delay associated with the diffusion of 'new' vorticity from the wall towards the pipe centreline (Maruyama *et al.*, 1976). In addition to this, there has been observed a third delay in the turbulence energy redistribution throughout the three orthogonal velocity components, implying anisotropy in the turbulence response (He & Jackson, 2000).

In this context, He & Seddighi (2013) analysed the mean flow response of an accelerating turbulent channel flow. That study revealed that the time response of the mean skin friction coefficient (C_f) followed a bypass-transition-like development. Additionally, it was determined that turbulence in the flow followed two transient stages. More recently,

(Guerrero *et al.*, 2021) performed a series of direct numerical simulations of accelerating turbulent pipe flows between two steady Reynolds numbers. The analysis of the mean flow dynamics of those DNS time series complemented previous investigations and revealed that a turbulent pipe flow following a rapid and linear acceleration exhibits four unambiguous stages; (I) inertial: a rapid increase in viscous forces and frozen turbulence behaviour; (II) pre-transition: a weak turbulence response in the near-wall region with a simultaneous fast reduction in the viscous forces; (III) transition: a proportional increase in viscous and turbulent forces at the inner region; and (IV) core-relaxation: a slow propagation of turbulence from the wall towards the wake region. Moreover, based on the FIK identity developed by Fukagata *et al.* (2002), Guerrero and co-workers derived several alternative expressions suitable to decompose the skin friction coefficient of an unsteady pipe flow into its dynamic contributions in integral form (Guerrero *et al.*, 2021, 2022a,b). This decomposition helps determine how the different terms of the mean momentum balance influence the mean WSS as a function of time.

The studies mentioned previously have provided substantial insight into the mean flow statistics relevant to accelerating flows. Nevertheless, the role of the LSM and the SSM during the flow development and how they contribute to the frictional drag is still elusive. Therefore, this investigation uses high- and low-pass Fourier filters to investigate how the large- (LSM) and small-scale motions (SSM) contribute to the generation and propagation of turbulence during the different stages undergone by a linearly accelerating flow. Furthermore, we use the FIK identity to identify how the large- and small-scale flow dynamics contribute to the temporal evolution of the frictional drag.

NUMERICAL DETAILS

Direct numerical simulations of an accelerating turbulent flow have been conducted using the Navier-Stokes solver Nek5000 (Fischer *et al.*, 2019). In this work, initially steady turbulent flow fields at a steady friction Reynolds number $Re_{\tau,0} \approx 500$ from Guerrero *et al.* (2020) are linearly accelerated by increasing their flow rate until they attain a value $Re_{\tau,1} \approx 670$. Subsequently, the flow remains at a constant flow rate until it fully develops and the universal laws of turbulence are attained. A cylindrical coordinate system has been adopted where r, θ and z are the radial, azimuthal and streamwise directions, respectively. The wall-normal direction is denoted as $y = R - r$. Similarly, the resolved velocity vector fields contain three orthogonal scalar components $U_r = -Uy$, U_θ and U_z whose fluctuating components are $u_r = -u_y$, u_θ and u_z, respectively. It is noteworthy that the "+0" or "+1" superscripts denote normalisation in viscous units at the initial

or final steady Reynolds numbers of the simulations, respectively.

The computational grid used in the present study was designed to have a suitable resolution at the highest Reynolds number attained. The computational grid used in the present investigation has a resolution $\Delta z^{+1} = 7.4$, $\Delta R\theta^{+1} = 6.3$, $y_{wall}^{+1} = 0.05$ and $y_{core}^{+1} = 7.5$. Further details about the simulation setup can be found in Guerrero *et al.* (2021).

RESULTS AND DISCUSSION

Time dependence of the Reynolds shear stress

Figure 1 depicts the Reynolds shear stress $\langle u_r u_z \rangle^{+0}$ decomposed into the large- and small-scale components using a wavelength threshold $\lambda \approx 2R$. This decomposition was performed using a high/low pass Fourier filter similar to Chin *et al.* (2014). The results show that during the inertial stage (figure 1a), the turbulence related to LSM and SSM is completely frozen. Throughout the pre-transitional stage (figure 1b) it is observed a stronger response in the large-scale turbulent motions, showing good agreement with the elongated streaks observed by He & Seddighi (2013) during the pre-transitional stage. During the early pre-transitional period, it is also interesting to note that there is a decay in the contribution of the small-scale structures to the Reynolds shear stress.

During the transitional stage (figure 1c), growth in both LSM and SSM turbulence is observed. However, a careful examination shows that within the inner region of the flow $y^{+0} \lesssim 100$, the SSM turbulence develops at a faster rate. It should be noted that within the core region of the flow, both SSM and LSM turbulence is nearly frozen. Finally, during the core-relaxation stage (figure 1d), the LSM and SSM contributions are nearly frozen at the near-wall region. However, similar rate of development in the LSM and SSM turbulence at the core region is observed.

Energy growth in the Reynolds shear stress

Figure 2 depicts the temporal evolution of the Reynolds shear stress' pre-multiplied co-spectra $\phi_{u_r u_z}^{+0}$ during a particular time location at the initial steady-state (figure 2a), the four transient stages (figures 2b−e) and the final steady-state (figure 2f).

It is noteworthy that the co-spectra by itself does not provide an accurate qualitative and quantitative indication in the energy growth. Thus, the difference in two consecutive spectrograms (i.e. $\phi_{u_r u_z}^{+0}(t + \Delta t) - \phi_{u_r u_z}^{+0}(t)$) provides a clearer picture of what scales of motion gain energy throughout the transient process. Figure 3 exhibits the results of that subtraction. For instance figure 3(a) is the result of subtracting $\phi_{u_r u_z}^{+0}(t^{+0} = 4.6) - \phi_{u_r u_z}^{+0}(t^{+0} = -1.2)$ (i.e. figure 2b - figure 2a). Moreover, it should be noted that the spectrogram has been subdivided
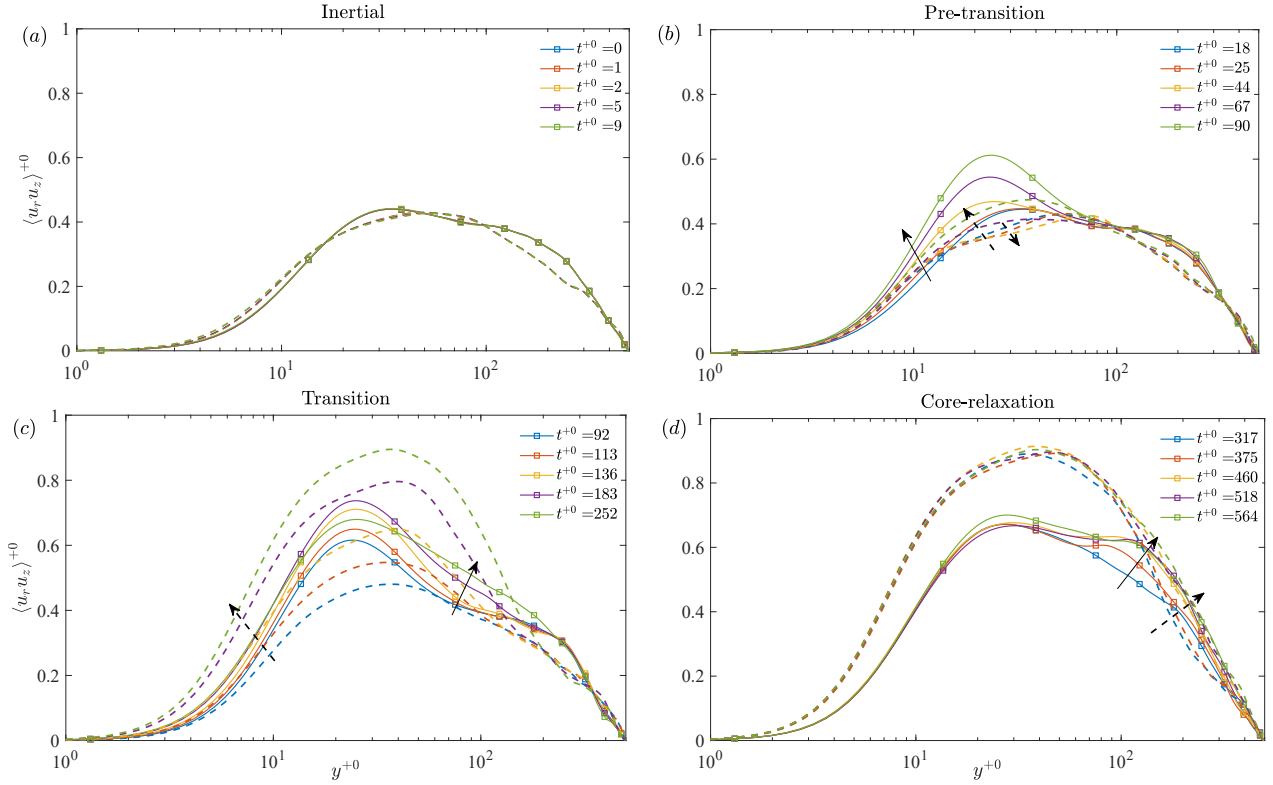
Figure 1. Time dependence of the large- (solid) and small-scale (dashed) components of the Reynolds shear stress during (*a*) the inertial, (*b*) pre-transition, (*c*) transition and (*d*) core-relaxation stages.
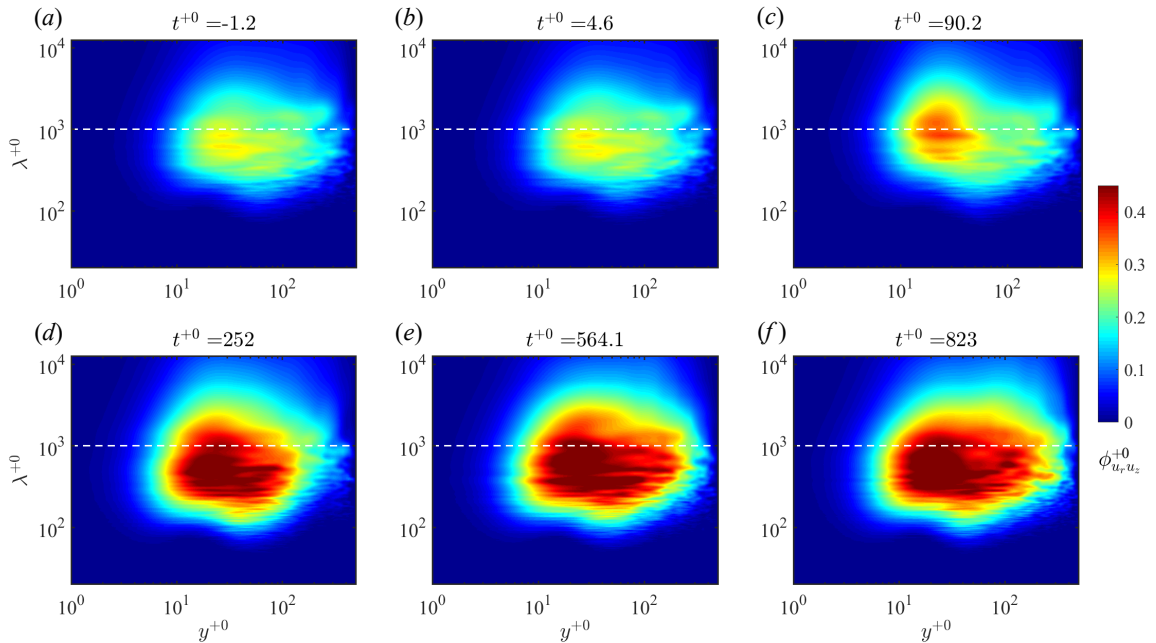

Figure 2. Temporal evolution of the Reynolds shear stress pre-multiplied co-spectra $\phi^+_{u_r u_z}$ throughout the different stages undergone by the flow: (*a*) Initial steady-state, (*b*) inertial, (*c*) pre-transition, (*d*) transition, (*e*) core-relaxation, (*f*) final steady-state. The white dashed line represents the threshold used to decompose the LSM and the SSM.

in six quadrants to better understand the regions and the length scales at which the energy growth occurs. In that context, the two vertical dashed lines subdivide the near-wall ($y^{+0} < 30$), overlap ($30 \lesssim y^{+0} \lesssim 200$) and wake ($y^{+0} > 200$) regions of the flow. Similarly, the horizontal line subdivide the scale ranges into into small- ($\lambda^{+0} \leq 1000$) and large-scale motions, where $\lambda^{+0} > 1000$ (i.e. $\lambda/R > 2$).

The results observed in figure 3(*a*) show that while the mean kinetic energy of the fluid increases
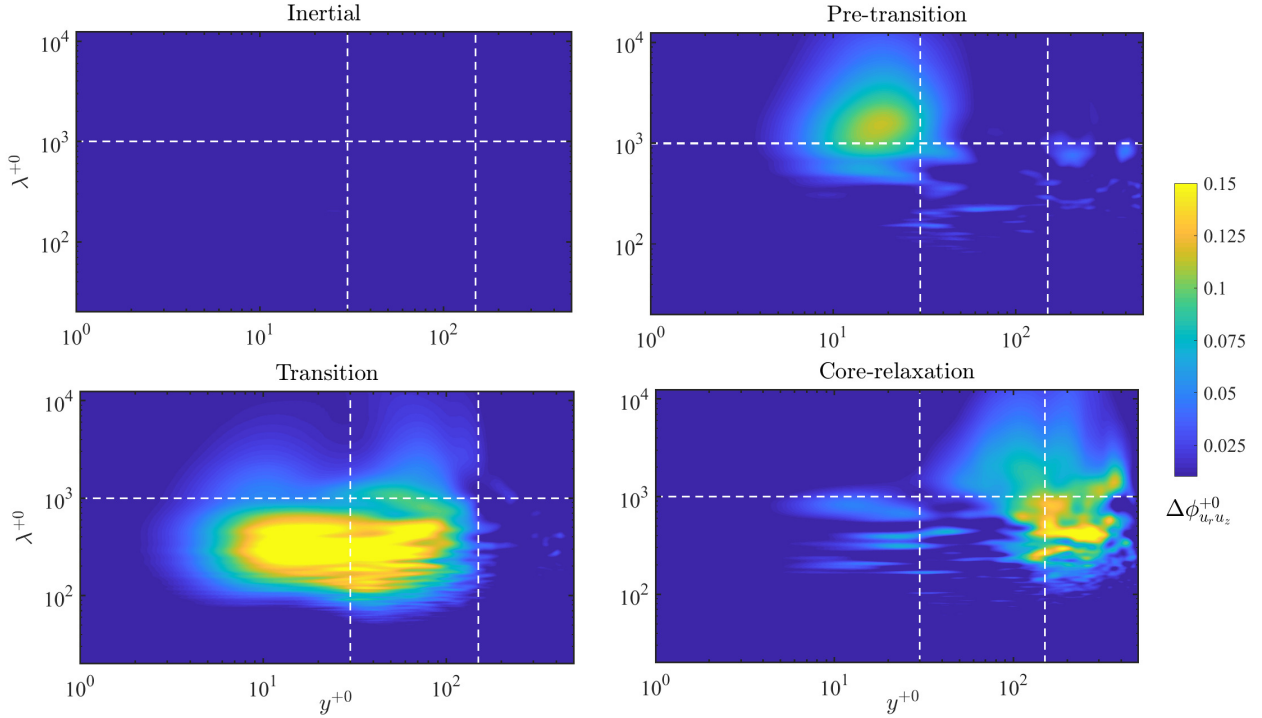
3

Figure 3. Energy growth in the Reynolds shear stress co-spectra throughout the four transitional stages underwent by an accelerating flow. The energy growth at each stage was obtained by subtracting two consecutive spectrograms from figure 2($a-e$).

during the flow excursion, the turbulent energy does not exhibit any significant changes throughout the pipe domain due to the delay in the turbulence response characteristic of the inertial period. These results agree with the 'frozen' turbulence observed during the early flow excursion observed in previous studies (Maruyama *et al.*, 1976; He & Jackson, 2000). Figure 3(b) shows that during the pre-transition, large-scale motions exhibit a considerable energy growth at the buffer region. This is in good agreement with the study by He & Seddighi (2013); Guerrero *et al.* (2022a) who observed the formation of elongated streaks at the near-wall region in accelerated channel and pipe flows, respectively.

The energy growth in the Reynolds shear stress throughout the transitional period is observed in figure 3(c). This figure reveals that most of the energy growth and the turbulence production at the inner region of the flow (i.e. $y^{+0} < 100$) occurs during the transition stage. Within this period, primarily small-scale structures are produced, agreeing with the production of 'new' turbulence occurring during this stage. Finally, figure 3(d) reveals substantial growth in the energy density at the wake region of the flow within the small and large-scale spectrum. Moreover, it is noted that there is a minor energy growth at the near-wall region during the core relaxation period.

Contribution of LSM and SSM into the wall friction

The FIK identity has been applied to the numerical data set used in this investigation following the alternative expression derived by Guerrero *et al.* (2021) for unsteady pipe flow. However, that expression was multiplied by $0.5\rho[U_b(t)]^2$ to express the frictional drag in terms of the wall shear stress rather than the skin friction coefficient. It is noteworthy that the turbulent component has been split into large- and small-scale contributions.

The results exhibited in figure 2(a) reveal that the LSM and SSM components of the turbulent term exhibit a substantially different response, especially during the inertial and the pre-transitional stages. The turbulent contribution associated with the small-scale components $\tau^T_{w,SS}$ seems nearly unchanged during the inertial and the pre-transitional stage. However, the large-scale turbulent contribution $\tau^T_{w,LS}$ only exhibits a frozen behaviour during the first stage and undergoes linear growth during the pre-transitional period. This is better observed in the zoomed view depicted in 2(b), where it is shown that $\tau^T_{w,SS}$ experience decay at $20 \lesssim t^{+0} \lesssim 60$, thereby suggesting a "laminarescent" behaviour of the flow during the pre-transitional stage.

Conclusions

Direct numerical simulation data sets of a rapidly accelerating turbulent pipe flow have been used to analyse the large- and small-scale contribu-
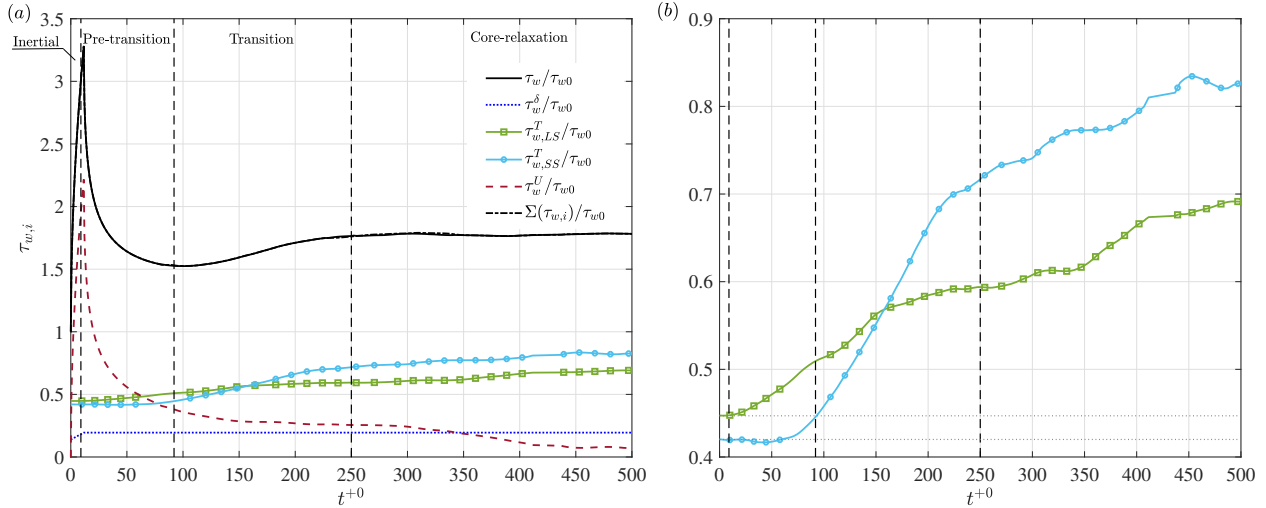
Figure 4. (*a*) FIK decomposition of the wall shear stress of an accelerating turbulent pipe flow. (*b*) Zoomed view of the turbulent term decomposed into the large- ($\tau^T_{w,LS}$) and small-scale contributions ($\tau^T_{w,SS}$).

tions to the Reynolds shear stress throughout the four transitional stages, characteristic of these flows.

During the inertial period, frozen turbulence behaviour is observed in both the LSM and SSM contributions.

The pre-transitional period exhibits a significant energy growth in the LSM range ($\lambda^{+0} \gtrsim 1000$) across the buffer region. These results are in good agreement with the observations by (He & Seddighi, 2013) who observed elongated streaks throughout this period. Moreover, the Reynolds shear stress and the small scale turbulent contribution of the wall shear stress $\tau^T_{w,SS}$ exhibit a slight temporary decay, suggesting a laminarescent trend during the early pre-transition. By the end of this period, small-scale turbulence starts gaining energy, consistent with the formation of new turbulent spots.

The transitional stage reveals an energy growth in both the large- and the small-scale range. However, the energy of small-scale turbulence grows at a higher rate during this period, which is consistent with the increase in the Reynolds number.

Finally, the core-relaxation period shows slight growth in large- and small-scale turbulence. The Reynolds shear stress co-spectra shows that most of this energy growth occurs at $y^{+0} > 200$.

REFERENCES

Chin, C., Philip, J., Klewicki, J., Ooi, A. & Marusic, I. 2014 Reynolds-number-dependent turbulent inertia and onset of log region in turbulent pipe flows. *J. Fluid Mech.* **757**, 747–769.

Fischer, P., Lottes, J. & Kerkemeier, S. 2019 Nek5000, Web page https://nek5000.mcs.anl.gov.

Fukagata, K., Iwamoto, K. & Kasagi, N. 2002 Contribution of Reynolds stress distribution to the skin friction in wall-bounded flows. *Phys. Fluids* **14**, L73–L76.

Guerrero, B., Lambert, M. F. & Chin, R. C. 2020 Extreme wall shear stress envents in turbulent pipe flows: spatial characteristics of coherent motions. *J. Fluid Mech.* **904**, A18.

Guerrero, B., Lambert, M. F. & Chin, R. C. 2021 Transient dynamics of accelerating turbulent pipe flow. *J. Fluid Mech.* **917**, A43.

Guerrero, B., Lambert, M. F. & Chin, R. C. 2022*a* Extension of the 1D unsteady friction model for rapidly accelerating and decelerating turbulent pipe flows. (in press)]. *J. Hydraul. Eng* .

Guerrero, B., Lambert, M. F. & Chin, R. C. 2022*b* Transient behaviour of decelerating turbulent pipe flows. Manuscript submitted for publication. *School of Mechanical Engineering, University of Adelaide* .

He, S. & Jackson, J. D. 2000 A study of turbulence under conditions of transient flow in a pipe. *J. Fluid Mech.* **408**, 1–38.

He, S. & Seddighi, M. 2013 Turbulence in transient channel flow. *J. Fluid Mech.* **715**, 60–102.

Maruyama, T., Kuribayashi, T. & Mizushina, T. 1976 The structure of the turbulence in transient pipe flows. *J. Chem. Eng. Jpn.* **9**, 431–439.

Reynolds, O. 1883 An experimental investigation of the circumstances which determine whether the motion of water shall be direct or sinuous, and of the law of resistance in parallel channels. *Phil. Trans. R. Soc. A* **174**, 935–982.